

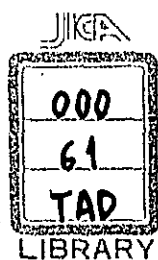
PRINCIPLES OF GEOPHYSICAL WELL LOGGING

TOSHINOBU ITOH

Japan Petroleum Exploration Corp.

1977

JAPAN INTERNATIONAL COOPERATION AGENCY



國業協力事業団	
受入 月日 84.5.23	000
登録No. 07039	61
	TAD


P. U. S.
C. I.

CONTENTS

24

1.	Introduction	1
2.	Conventional electrical log	2
3.	Fundamental formula to drive a formation porosity and water saturation from well log data	5
4.	R_w Calculation by the use of Spontaneous potential log	7
5.	The improvement of S_w calculation by studying fluid distributions near close to the hole-wall in the permeable formation	10
6.	Micro log	14
7.	Guard electrode log	16
8.	Micro-latero log	18
9.	Induction log	18
10.	Sonic log	20
11.	Natural gamma-ray log	24
12.	Formation density log (Gamma-gamma density log)	25
13.	Neutron log	29
14.	Log interpretation in shaly sand	31
	1) PSP method	32
	2) Recent S_w equation for shaly sand	33
	3) V_{sh} calculations based on the material balanced equation by the help of data given by the sonic log, formation density log and neutron log	33

JICA LIBRARY



1014902[9]

6168

TEL. 6168

P. U. S.
C. I.

1. Introduction

It is more than 50 years past since geophysical well loggings has been introduced into the oil industry by Conrad Schlumberger(France) at 1927. On the early stage of those well logging techniques, only one formation resistivity measured by so called Normal resistivity measuring method and a spontaneous potential (SP) were available in the practical uses, and those curves were used as a reference of qualitative geological interpretations of the formation such as resistivity discrimination of the formation or the depth co-relation of the formation between two adjoining wells.

On 1940 age, many kinds of scientist starting G.E. Archie have developed the quantitative relationships between the formation resistivity and the physical parameters of formation, i.e., porosity, water saturation in the pore space, resistivity of formation water, etc. On the results of those fundamental research of log interpretation, many kinds of logging method which measure such physical parameter of formation have been developed continuously, especially a rapid improvement on electronics technology after the 2nd world war helped to the realization of high quality logging tools such as Induction-electrical log, Micro log, Latero and Microlatero log, Sonio log, Neutron log, Gamma-gamma density log (Formation density log), etc., and the log interpretation techniques have also improved in connection with the improvement of those new logging equipments. Moreover, the data processing techniques using the computer, which was introduced into the logging techniques on 1960 age, promoted the digitization of well log data and the precisness of the log interpretations.

At the present day, the geophysical well logging can not only calculate the formation porosity and water saturation which are important factors on the calculation of oil and gas reserves, but also determine the formation materials with the help of material balanced equations composed with physical characteristics of the formation and the log data given by several logging methods. Beside those, many kinds of new logging method which are based on the direct analysis of formation materials have been proposed into the actual logging operations continuously up to data. Those are Nuclear magnetism log, Spectral gamma-ray log, Fluorescence X-ray log, Neutron activation log, Neutron life time log, etc., and some of them are in the practical uses at the present day.

2. Conventional Electrical Log

This is a most classical method in the well logging which measure the formation resistivity. Electrical log measures a formation resistivity and a spontaneous potential (mentioned at later on) by means of so called Normal resistivity measuring method (Normal method) shown at Fig. 1 (a).

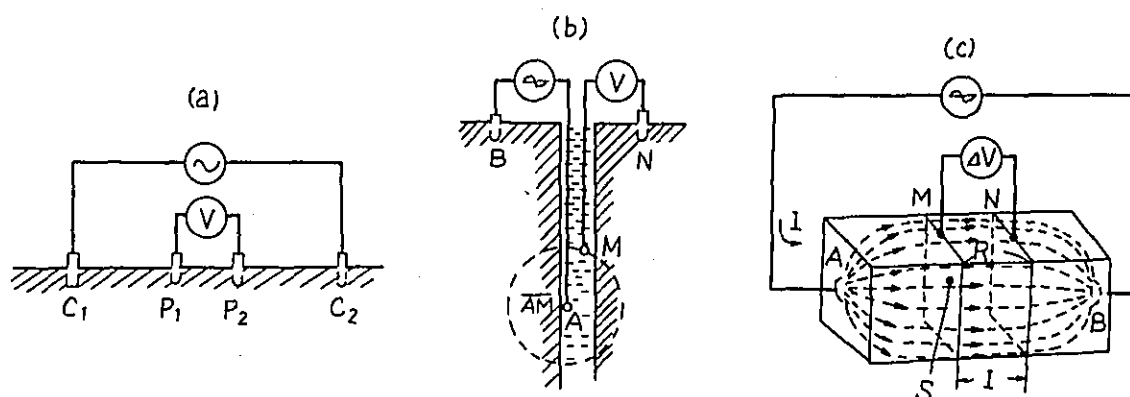


Fig. 1 Normal Resistivity Measuring Method.

Before the explanation of this method, the principle of resistivity measurement of materials will be explained by the use of Fig. 1 (c). Potential difference between two electrodes \$M\$ and \$N\$ will be given by following equation.

$$\Delta V = RI$$

Where, ΔV : potential difference between two electrodes \$M\$ and \$N\$.

R : resistance of the sample held between those electrodes.

I : current passing through the sample.

If a current passing through electrode \$M\$ distributes in uniformity all over the surface, a density of current on this surface will be given as follows.

$$i = \frac{I}{\int^S ds} = \frac{I}{S}$$

Where, $\int^S ds = S$ is the cross section of surface at electrode \$M\$ and \$i\$ is a current density. Since a voltage drop per unit volume of sample is given by the product of resistivity of sample (ρ) and current density (i), the total voltage drops over the sample held between two electrodes will be given as follows.

$$\Delta V = RI = \int_0^l \rho i \, dx = \rho \frac{I}{\int_s ds} \int_0^l dx = \frac{I}{S} \rho l$$

Where, l is a distance between two electrodes and it is, then, understood that the relationship between R and ρ is given by $R = \frac{l}{S} \rho$. Therefore, if the measuring conditions such as length, cross section of the sample and the current are kept at constant during the measurement, ρ value can be driven by ΔV value directly. On the normal method shown at Fig. 1 (a), when the material surrounding the probe have a resistivity of ρ , a current density at the surface of sphere with radius r will be given as :

$$i = \frac{I}{\int_s ds} = \frac{I}{4\pi r^2}$$

Then, a voltage drop between current electrode A and potential electrode M can be driven as same manner as the case of core resistivity measuring system, i.e.,

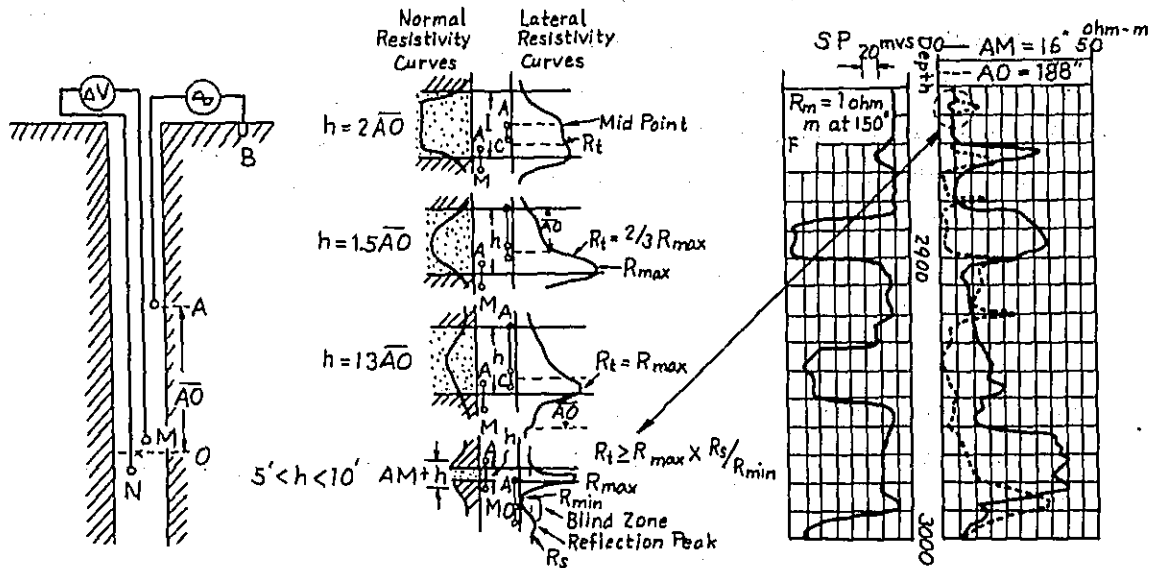
$$\Delta V = \int_{AM} \rho i \, dr = \int_{AM} \frac{I}{4\pi r^2} \rho \, dr = \frac{I}{4\pi} \frac{I}{AM} \rho \dots \dots \dots (1)$$

Where, \overline{AM} is the distance between electrode A and M. Therefore, the formation resistivity can easily be driven from ΔV value directly if the current applying into the formation radiated from electrode A is kept at constant during the measurement.

In the practical cases, materials surrounding a logging probe distribute as such manner as mud column, mud invaded zone (the zone of which a formation fluids are replaced with the mud filtrate water) and uncontaminated zone (natural zone) from the surface of probe to the inside of formation. Therefore, the readings of normal method do not always give the truth value of formation resistivity. The longer the spacing of \overline{AM} gives more close value to the true formation resistivity, because a volumetric ratio between the total volume of investigation area of the normal method (inner space of sphere with the radius \overline{AM}) and the area which is occupied by the mud column and mud invaded zone will decrease in connection with the increase of \overline{AM} spacing. Meanwhile, the normal method has a fault that the resistivity curve becomes hollow in front of the resistive formation having the bed thickness less than \overline{AM} spacing as shown in Fig. 2 (b), and this means that the resolution of normal method for thin

bed thickness decreases in connection with the increase of \overline{AM} spacing.

Lateral resistivity measuring method (lateral method) which measures a formation resistivity by means of 3 electrodes inserted into the hole (a current electrode A and potential electrodes M and N) as shown in Fig. 2 (a) was developed for covering such shortcomings on the normal method.



(a) Lateral resistivity measuring method. (b) Some rule to get R_t values from lateral curve. (c) Example of Conventional electrical log.

Fig. 2 Conventional Electrical Log.

Since the spacings of electrodes A, M and N on the lateral method are such arranged that the relationship of $\overline{AO} \gg \overline{MN}$ is always held, where, point O is a midpoint between electrode M and N, the potential drop between electrodes M and N will be given by the following equation.

$$\Delta V = \int_{\overline{AM}}^{\overline{AN}} \frac{\rho I}{4\pi r^2} dr - \int_{\overline{BM}}^{\overline{BN}} \frac{\rho I}{4\pi r^2} dr \approx 4\pi \frac{\overline{MN}}{2} \cdot \frac{1}{\overline{AO}^2} \cdot \rho \dots (2)$$

Although the lateral resistivity curve shows rather complicated shape in comparison with the normal curve, the details of curve for the formation having thin-bed thickness are much superior than the one of normal curve as shown in Fig. 2 (b). Moreover, the investigation area of this method (inner space of sphere with the radius \overline{AO}) is much larger than the one of normal method. This means that the lateral resistivity is less influenced by the hole conditions in comparison with the normal resistivity. Some rules to get R_t (true resistivity) value from lateral resistivity curves are also shown in Fig. 2 (b).

3. Fundamental Formula to Drive a Formation Porosity and Water Saturation from Well Log Data

At the early stage of well logging, electrical log data were mainly used as a help of qualitative geological interpretations such as lithological discrimination in accordance with formation resistivities or depth correlation of the formation between adjoining two wells. On the 1940 age, G.E. Archie introduced the quantitative relationship between the formation resistivity and physical parameters of formation such as porosity, resistivity of formation water and water saturation in a pore space of the formation. On the Archie's experiments, a resistivity of core samples whose pore space is fully filled by brine water increases gradually in accordance with the increase of oil concentration in a formation fluids, then the following equation has been driven empirically.

$$S_w = (R_o / R_t)^{1/2} \dots\dots\dots(3)$$

Where, R_o : formation resistivity at the first stage (a pore space is fully filled by the brine water).

R_t : formation resistivity when a water saturation of the formation liquid is S_w .

S_w : water saturation of formation liquid.

Moreover, Archie also defined that the resistivity of core sample whose pore space is fully filled by the brine water is proportional to the resistivity of brine water, and ratio between the formation resistivity and the resistivity of formation water holds constant on the clean formation (any mudstone is not included), i.e.,:

$$F = R_o / R_w \text{ or } R_o = F R_w \dots\dots\dots(4)$$

Where, F : formation resistivity factor.

R_w : resistivity of formation water.

In comparison with this equation and the general formula of the relationship between the resistivity and resistance of material, i.e., $R = \frac{1}{S} \rho$. F is in correspondence with $\frac{1}{S}$ on the equation of $R = \frac{1}{S} \cdot \rho$, in other words, F is a function of cross section and effective length of the conductive fluid included in the unit volume of formation. Therefore, it

is easily understood that a formation resistivity factor might have some relations with the formation porosity, (ϕ), then, Archie drove the following equation between F and ϕ .

$$F = a / \phi^m \dots\dots\dots (5)$$

Where, a is a constant and m is a compaction factor of the formation. In the practical cases, $F = a / \phi^m = 0.62 / \phi^{2.15}$ is used on the well compacted sandstone formation normally. But, when the equation of $F = 1 / \phi^2$ is applied into the well compacted sandstone instead of $F = 0.62 / \phi^{2.15}$, the value of ϕ will not much differ from the one given by the equation of $F = 0.62 / \phi^{2.15}$, then, the following equation will be formed with the combination of equations (3), (4) and $F = 1 / \phi^2$, for clean formation.

$$1/R_t = \frac{(S_w \phi)^2}{R_w} \dots\dots\dots (6)$$

This equation indicates "Since an oil and rock have the infinitive resistivity, the resistivity of formation is only proportional to the resistivity of formation water and its effective volume (ϕS_w)". On the early stage of well logging, it was too short informations to drive S_w values by the use of the equation (6) because only the electrical log was available in the practical use.

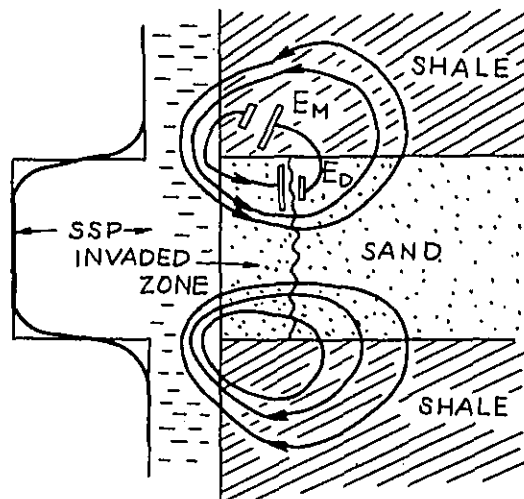


Fig. 3 Principle of Spontaneous Potential

4. R_w Calculation by the use of Spontaneous Potential Log

Spontaneous potential log measures the potential difference between the electrode inserted into a hole and the surface electrode continuously. It is well known that the potential when the down-hole electrode is in front of the pervious formation differs from the one when the electrode is in front of the unpervious formation, and this potential difference is called SP value. Therefore, geological discriminations between the pervious formation and the unpervious formation can be achieved by the use of this SP value. This spontaneous potential is caused by the electro-chemical e.m.f. appeared at the boundary between a permiable formation and unpervious mudstone (shale) as shown in Fig. 3. The electro-chemical e.m.f. can be devided into following two components, the one which appears at the surface where two electroytes having the different ion concentrations are contacted in a pervious formation is called Electro-diffusion potential, and another which appears at the contact of mud - mudstone - formation water is called Electro-membrane potential.

o Electro-diffusion potential E_D

When two electroytes having the different concentration of active ion contact in a pervious formation, a diffusion of active ion occures between those two electroytes. If those two electroytes are consisted of a NaCl water, the electro-chemical e.m.f. caused by the movements of active ion is due mainly to the diffusion of Cl^- ion from the more concentrated electroyte to the less concentrated one. Then, E_D will be represented by a following equation.

$$E_D = \frac{RT}{F} (2t^{-1} - 1) \log \frac{a_w}{a_{mf}} \dots\dots\dots(7)$$

Where, $\frac{RT}{F}$: constant depending on the temperature.

t^{-1} : transfer efficiency of Cl^- ion.

a_w : activity of uncharged ion in the formation water.

a_{mf} : activity of uncharged ion in the mud filtrate water.

o Electro-membrane potential E_M

Since the surface of mudstone is covered by a negative charge, a

diffusion of plus ion will occur between two electrolytes which are faced to each other through a mudstone in the middle of them. The electro-chemical e.m.f. caused by this ion movement is also given as similar form as equation (7).

$$E_M = -\frac{RT}{F} \log \frac{a_w}{a_{mf}} \dots\dots\dots (8)$$

Since E_D and E_M have a same polarity as shown in Fig. 3, the total e.m.f. of spontaneous potential is represented as follows.

$$E_{SP} = E_D + E_M = -K \log \frac{a_w}{a_{mf}}$$

Where, $K = -2.3 \frac{RT}{F} 2t^{-1} = 70.7 (460 + T_f) / 538,$

If the electrolyte includes Mg^{++} , Ca^{++} , SO_4^{--} , HCO_3^{--} other than Na^+ , Cl^- ion, the correction factors given in Table I should be taken in account on the calculation of ion activity of the electrolyte.

Table I : Correction factor of ion activity
(equivalent to the activity of Na^+ , Cl^- ion)

Ca^{++} ; 0.95	SO_4^{--} ; 0.5
Mg^{++} ; 2.0	CO_3^{--} ; 1.26
	HCO_3^{--} ; 0.27

Example : Components of electrolyte ; NaCl : 25,000 ppm, $CaCO_3$: 2,000 ppm.

Ion activity (equivalent to NaCl electrolyte)

$$\begin{aligned} a &= 25,000 \left(\frac{Na}{NaCl} \times 1 + \frac{Cl}{NaCl} \times 1 \right) \\ &+ 2,000 \left(\frac{Ca}{CaCO_3} \times 0.95 + \frac{CO_3}{CaCO_3} \times 1.26 \right) \\ &= 27.272 \text{ ppm} \end{aligned}$$

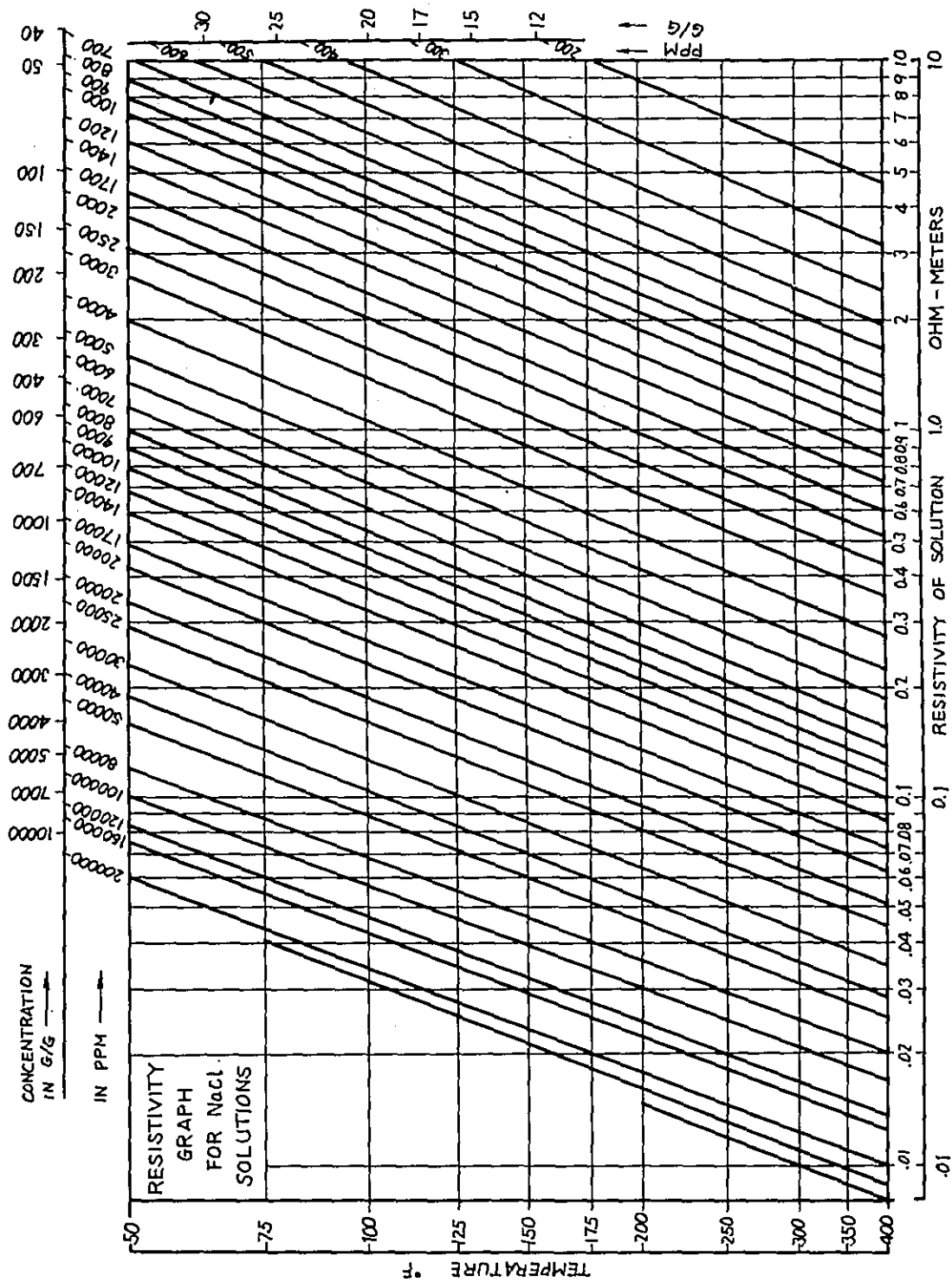


Fig. 4 Chart for Driving the Resistivity of Electrolyte.

When the resistivity of electrolyte is held within $0.03 R_F$ 0.3 ohm-m (at 75°F), it is considered that the resistivity of electrolyte will be counter proportional with an ion activity, accordingly the concentrations of NaCl in the electrolyte as shown in the chart of Fig. 4. Then, the equation (8) can be re-written as follows.

$$E_{SP} = -K \log \frac{a_w}{a_{mf}} = -K \log \frac{R_{mf}}{R_w} \dots\dots (9)$$

As a nature of SP logging method, SP value represents the product of mud resistance in the hole - $R_{(mud)}$ - and current passing through the closed loop - i - formed at the boundary between the mudstone and permeable formation as shown in Fig. 3. Accordingly, SP is given by the following equation.

$$SP = R_{(mud)} \times i = R_{(mud)} \frac{E_{SP}}{R_{(mud)} + R_{(shale)} + R_{(invaded\ zone)} + R_{(natural\ zone)}}$$

Where, $R_{(mud)} + R_{(shale)} + R_{(invaded\ zone)} + R_{(natural\ zone)}$ is a resistance of this closed loop. Therefore, SP does not always coincided with E_{SP} .

But, in the practical case, the relationship of $R_{(mud)} \gg R_{(shale)}$,

$R_{(invaded\ zone)}$, $R_{(natural\ zone)}$ could be held when the bed thickness of permeable formation (e) is quite larger than the diameter of hole (D), i.e., $e > 10D$. Then, SP value represents the equal value of E_{SP} in this case, and this SP is called as SSP. Therefore, equation (9) can be re-written as follows.

$$SSP = E_{SP} = -K \log \frac{R_{mf}}{R_w} \dots\dots\dots (10)$$

Since R_{mf} can be measured by the use of sample of mud filtrate water directly, R_w will be driven from SP log data by the use of equation (10).

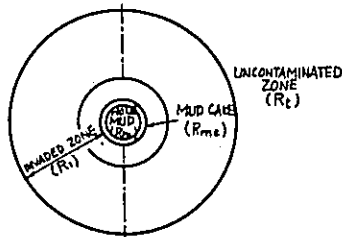
5. The Improvement of SW Calculation by Studying Fluid Distributions Near Close to the Hole-wall in the Permeable Formation

Although the conventional electrical logging can measure 16" and 64" Normal resistivity, 18'8" Latral resistivity and SP simultaneously, Sw calculations based on the equation (6) can not be achieved only by those data given by the electrical log because of the lack of porosity informations.

On rotary drilling system, a hole is drilled by the rotating bit which is connected in the lower extreme point of drill pipe. Cuttings of formation cut off by this bit are brought up to the surface with the help of drilling mud which is circulated between the drill pipe and the drilled hole. This

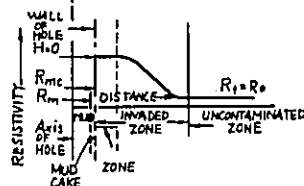
drilling mud has also a role of suppressing a blow out of formation fluids, in other words, the mud weight is normally so controlled that the hydrostatic pressure of mud is always higher than the one of formation fluids. Therefore, the mud filtrate water will invade into the permeable formation and solid materials included in the mud will pile up at the wall surface of the formation. When those solid materials are piled enough up to some thickness and pressed compactly (solid materials piled up at the surface of formation is called mud cake), the further migration of mud filtrate water is stopped by this mud cake. And then, fluid distributions in the permeable formation will be in balanced condition. Fig. 5 shows fluid distributions in the permeable formation near close to the hole-wall. The upper is the one for low hydrocarbon bearing formation and the lower is the one for high hydrocarbon bearing formation, and resistivity distributions

Horizontal Section Through a Permeable Water - Bearing Bed

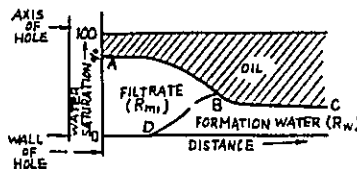


(a) Invasion in a water bearing formation.

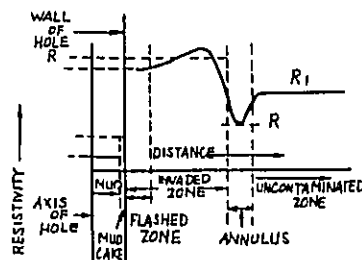
Radial Distribution of Resistivities ($R_{mf} \gg R_w$)



Radial distribution of Fluids in the Vicinity of the Bore Hole (qualitative)



Radial Distribution of Resistivities ($R_{mf} \gg R_w$)



(b) Invasion in an oil bearing formation.

Fig. 5 Fluid Distributions in the Permeable Formation.

corresponding to each case are also shown in the figure individually. On the low hydrocarbon bearing formation, fluid distributions in the permeable formation are as follows from the surface of hole-wall to the inside of the formation, i.e., mud column, mud cake, the zone where the liquids in apore space are fully replaced by the mud filtrate water (called as flushed zone), the zone where liquids in a pore space are mixture of formation water, hydrocarbons and mud filtrate water (calles as invaded zone) and the zone where formation liquids are not polluted by any mud filtrate water (called as uncontaminated or natural zone). The boundary of those zone and their extensions are not so clear as shown in the figure in practical cases. On the high hydrocarbon bearing formation, formation fluids in the flushed zone are not fully replaced by the mud filtrate water and some hydrocarbons (oil and gas) still exist in this zone generally, moreover, the zone which has higher water saturations than the one of natural zone exists between the mud inveded zone and the natural zone (called as annulus). This phenomenon is mainly caused by the difference of diffusion efficiency between oil and gas and formation water, in other words, the diffusion rate of hydrocarbons is normally much faster than the one of formation water on the high hydrocarbon bearing formation, then the formation water will be accumulated in front of the natural zone temporary. The existence of this annulus is some times proved by the data of Induction log.

Water saturation at the flushed zone Sx_o ($Sx_o = 1 - R.O.S.$, where, R.O.S. is called as residual oil saturation) can be given as same forms as the equation (3).

$$Sx_o = (Rx_o / Rx_{oo})^{1/2} \dots\dots\dots (11)$$

Where, Rx_o : resistivity of flushed zone whose formation fluids are fully replaced with the mud filtrate water.

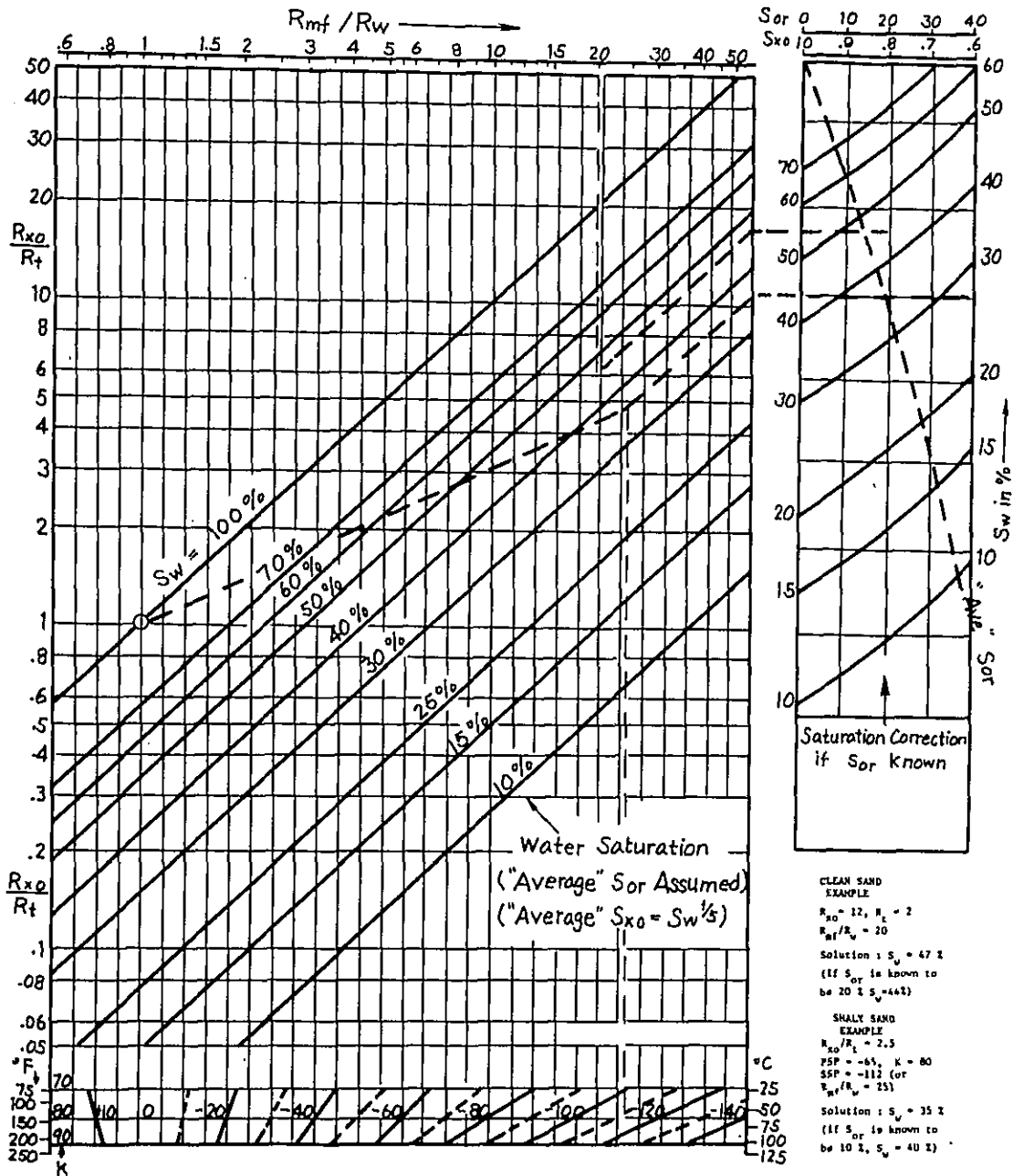
Rx_{oo} : resistivity of flushed zone when some residual oil exists in apore space.

The formation resistivity factor will be given by the following equation.

$$F = \frac{Rx_o}{R_{mf}} - \frac{1}{\phi^2} \dots\dots\dots (12)$$

On combining with equations (11), (12) and (6), a following equations can be driven :

SATURATION DETERMINATION (RATTO METHOD)



Procedure : For clean sands plot the ratio R_{xo}/R_t against R_{mf}/R_w to find water saturation at "average" residual oil saturation ($S_{xo} = S_w^{1/5}$). The SP can be used instead of R_{mf}/R_w assuming $PSP = -K \log R_{xo}/R_t$ (no activity correction is made).

For shaly sands plot R_{xo} against PSP. Draw a line through this point and the circle where $R_{mf}/R_w = R_{xo}/R_t = 1$. Extend line to intersect the value of SSP (or R_{mf}/R_w) to find water saturation at "average" S_{or} . Use diagram at right to correct S_w if S_{or} is known.

Fig. 6 SSP - R_{xo}/R_t - S_w Calculation Chart.

$$\phi = (R_{mf}/R_{x_{oo}})^{1/2} \cdot \frac{1}{S_{x_o}} \dots\dots\dots (13)$$

and
$$\frac{R_{mf}}{R_w} = \frac{R_t}{R_{x_{oo}}} \times \frac{S_{x_o}^2}{S_w^2}$$

When the lower equation is transferred into the equation (10), the following SP equation will be gained.

$$SSP = -K \log \frac{R_{mf}}{R_w} = -K \log \frac{R_{x_{oo}}}{R_t} - 2K \log \frac{S_{x_o}}{S_w} \dots\dots (14)$$

Above two equations (13) and (14) are fundamental formula of log interpretation based on the resistivity informations. Therefore, ϕ and S_w can be calculated from those equations with the help of data given by Electrical log, Induction log and Latero log (R_t), SP log (R_w), Micro log or Micro-latero log (R_{x_o}) etc. (those logging methods will be explained at later on).

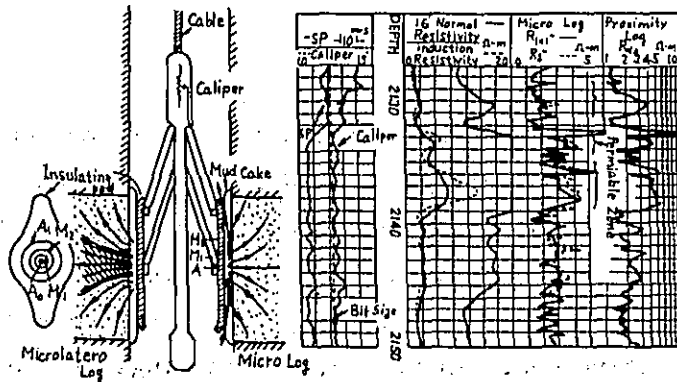
Fig. 6 is a S_w calculation chart based on the equation (14), where

$$S_{x_o} = S_w^{1/5} \text{ is applied.}$$

6. Micro Log

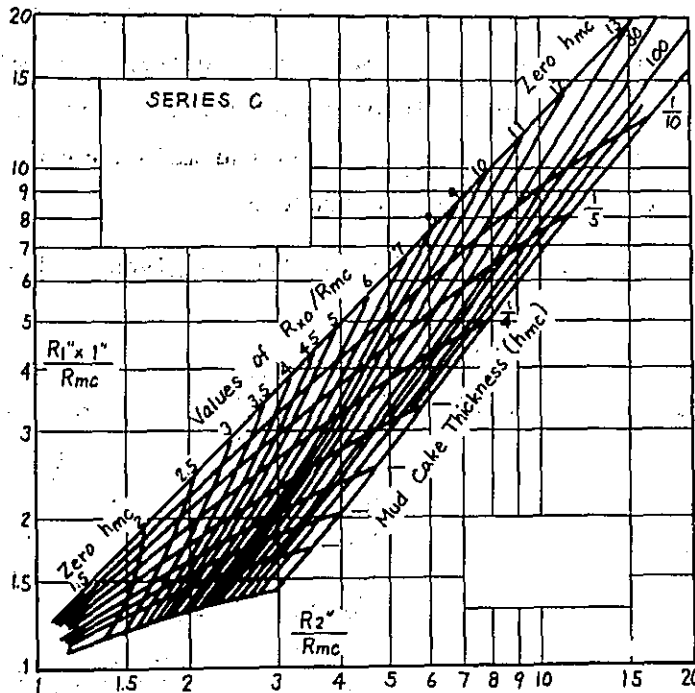
Micro log measures the resistivity of a small volume of formation near close to the hole-wall by applying an insulation pad which encloses the button electrodes arranged in Normal and Lateral method having a small spacing of 1" as shown in Fig. 7. On this method, a normal resistivity measured by the spacing AM of 2" (called as R_2 "), a lateral resistivity measured by the spacing A and M, N of 1" (called as R_{1x1} "") and a caliper (hole diameter) are recorded on the oscillograph film simultaneously.

The resistivity of flushed zone is normally higher than the one of mud cake as shown in Fig. 5. Since the investigation depth of R_2 " is deeper than the one of R_{1x1} "", the readings of micro log show R_2 " > R_{1x1} " in front of the permeable formation (this display of micro log is called as "positive separation"). This positive separation and mud cake thickness measured by the caliper log have key informations of the detection of permeable formation. Fig. 8 is a chart to get R_{x_o} value from R_2 " and R_{1x1} ".



(a) Current distributions (b) Example of Micro and Micro-latero log.
of Micro and Micro-latero log.

(Fig. 7 Principle of Micro and Micro-latero Log.



For hole sizes other than 8", multiply $R_{1'' \times 1''} / R_{mc}$, by the following factors before entering the chart:

1.15 for 4 3/4 inch-hole, 1.05 for 6-inch hole, 0.93, for 10-inch hole.

NOTE : An incorrect R_{me} , will displace the points in the chart along a 45° line. In certain cases this can be recognized when the mud cake thickness is different from direct measurement by the micro-caliper. To correct, move the plotted point at 45° to intersect the known h_{mc} . For this new point read R_{xo} / R_{mc} , from the chart and $R_{2''} / R_{mc}$, from the bottom scale of the chart.

R_{xo} / R_{mc} , times R_{mc} , equals R_{xo} .

Fig. 8 R_{xo} Chart by the Use of Micro Log.

7. Guard Electrode Log (Latro Log)

When the resistivity contrast between mud and formation is extremely large, in such case as the well which is drilled by a high conductive mud (sea water based mud) or a reservoir which is consisted of high resistive rocks, almost all the current radiated from electrode A on the electrical log does not enter into the formation but escapes to the surface passing through a low resistive mud. Therefore, the readings of the electrical log will deviate from a truth value of formation resistivity strongly. Guard electrode log has auxiliary current electrodes of A_1 and A_1' which are set at upper and down side of main electrode A_0 with a vertical symmetry as shown in Fig. 9. Since those auxiliary electrodes are held at little higher potential than the one of main electrode A (some polarity), the current radiated from the main electrode flows into the formation with a disc shape as shown in Fig. 9 compulsory. In other words, the auxiliary current radiated from electrodes A_1 and A_1' forces the main current to be a disc shape with the thickness of belt electrode A_0 .

The resistivity measured by this system is given as $R = \frac{V_0}{I_0}$,

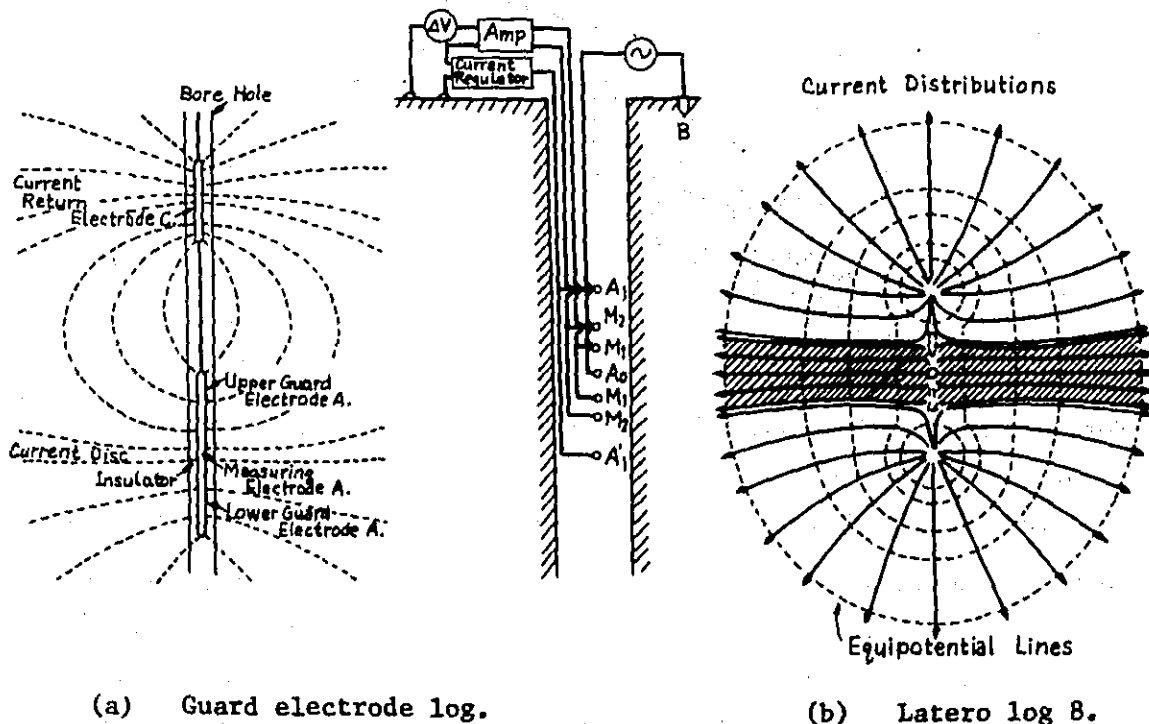


Fig. 9 Principles of Guard Electrode Log.

where, V_0 is a potential difference between the main electrode A_0 and the surface electrode and I_0 is a current radiated from the main electrode A_0 . When the bed thickness is larger than the wideness of belt electrode A_0 ,

relation-ship between the measured resistivity by this method and the one of materials surrounding the probe can be written as following equation.

$$\bar{R}_a = \frac{V_o}{I_o} = G_m \rho_m + G_i \rho_i + G_t \rho_t \dots \dots \dots (15)$$

Where, G_m, G_i, G_t : geometrical factor of equipment for mud column, invaded zone and uncontaminated zone.

ρ_m, ρ_i, ρ_t : resistivity of individual materials.

Approximate values of those G_m, G_i, G_t are as follows (given by R.J. Schopper),

$$G_m = \frac{1}{2\pi l_o} \log \frac{r_m}{r_e}, \quad G_i = \frac{1}{2\pi l_o} \log \frac{r_i}{r_m}, \quad G_t = \frac{1}{2\pi l_o} \left(\log \frac{1}{2r_i} + 1 \right)$$

Where, l_o : wideness of belt electrode A_o .

r_e : diameter of belt electrode A_o .

r_m : hole diameter

r_i : diameter of mud invaded zone.

l : length of auxiliary electrodes A_1 and A_1' .

Therefore, the resistivity measured by this method will be expressed as.

$$\bar{R}_a = \frac{1}{2\pi l_o} \left[\rho_m \log \frac{r_m}{r_e} + \rho_i \log \frac{r_i}{r_m} + \rho_t \left(\log \frac{1}{2r_i} + 1 \right) \right] \dots \dots \dots (16)$$

From this equation, it is understood that the larger resistivity contrast between $\rho_m, \rho_i,$ and ρ_t gives the more close value to the true formation resistivity on the guard electrode log, because the relation-ship of

$\rho_m \log \frac{r_m}{r_e} + \rho_i \log \frac{r_i}{r_m} \ll \rho_t \left(\log \frac{1}{2r_i} + 1 \right)$ will more and more be satisfied in connection with the increase of resistivity contrast.

Latero log 8 which was developed by Schlumberger Corp. (France) has same effect as the guard electrode log but has a different mechanism of current focusing system. Principle of this method is shown in Fig. 9 (b), i.e., another electrodes M_1 and M_2 are set at the mid-point between current electrodes A_o and A_1 (M', M_2' on a down side), and the current radiated from the electrodes A_1 and A_1' is such controlled that a potential difference

between electrodes M_1 and M_2 is always kept at zero volt by means of electronics circuit. Therefore, the current radiated from main electrode A_0 will be forced to have a disc shape having the thickness of equal distance between M_1 and M_1' as shown at right side in the figure. In other words, the zero potential difference between electrode M_1 and M_2 (namely, M_1' and M_2') means that any current radiated from electrode A_0 can not cross the wall of such zero potential.

8. Micro-latero Log

Micro-latero log measures R_{x_0} by means of short electrode spacing of latero log. The arrangements of measuring electrode are followed by the one of latero log 8 but the spacing of those electrode is about 1" as shown at left side in Fig. 7 (a).

On this logging system, the resistivity of flushed zone is given in the logarithmic scale directly as shown in Fig. 7 (b) when the mud cake thickness is less than 3/4 inch.

9. Induction Log

The logging systems which inject a measuring current into the formation passing through a conductive mud can not be applied into the well which is drilled by the none conductive mud such as oil base mud well or air drilled hole. Induction log measures a formation conductivity by means of electro-magnetic force as shown in Fig. 10. When a formation is excited by the alternative electro-magnetic force having a constant intensity (about 20 K Hz), an eddy current is induced inside the formation, and the intensity of this eddy current is proportional with the conductivity of formation, a receiver coil of induction log receives the vector sum of following two components, the one is a part of main electro-magnetic force radiated from transmitter coil (idle component), and the another is a part of electro-magnetic force which is induced by the eddy current flowing in the formation (signal component). Such receiver signals are sent to the electronics block in the down hole probe, and then the signal is separated into those two components on this block individually.

Since a polarity and intensity of the vector of signal component can be controlled by the direction of coil spiral and turn ratio between transmitter coil and receiver coil as shown in Fig. 11 (a), the responses of induction log can be cancelled out for some distance from the surface of

probe on radial direction by the use of additional coils. Fig. 11 (b) shows the radial responses of Schlumberger 6 FF 40 (consisted of 6 coils, and spacing between main transmitter coil and receiver coil is 40").

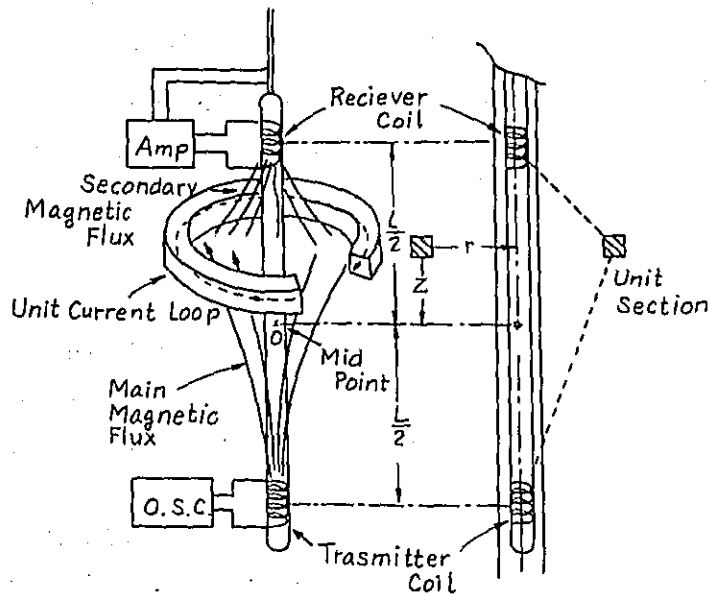
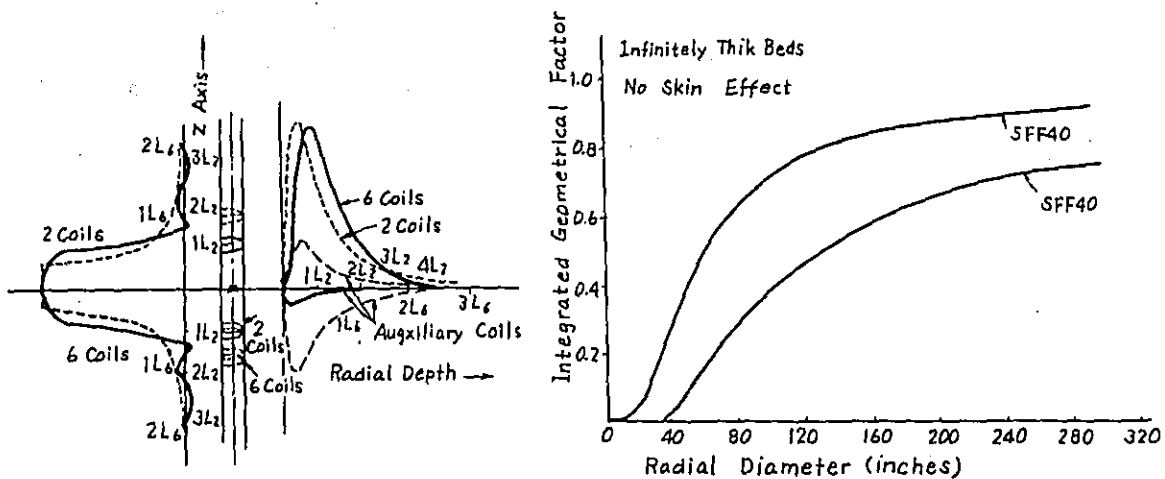


Fig. 10 Principle of Induction Log.



(a) Geometrical factor of induction log (b) Integrated geometrical factor of Schlumber 5FF40 and 6FF40 induction log.

Fig. 11 Geometrical Factor of Induction Log.

The formation conductivity measured by the induction log is given by following equation.

$$C = G_m C_m + G_i C_i + G_s C_s + G_t C_t \dots \dots \dots (17)$$

On the 6 FF 40 induction log, a relationship of $G_m, G_i \ll G_t$ is also held when the bed thickness of formation is larger than the spacing of main coils as shown in Fig. 11. Therefore, it is understood that the 6 FF 40 induction log gives a very close value to the true formation conductivity for the relatively wide range of hole and formation conditions.

The standard equipment of 6 FF 40 induction log can also measure 16" short normal resistivity and SP in addition to the induction conductivity simultaneously.

10. Sonic Log

Sonic log measures a velocity of elastic wave in the formation. The principle of this method is shown in Fig. 12, a sonic pulse radiated from the sonic transmitter (inherent vibrating frequency : about 20 KHz, repetition rate of sonic pulse : 10 20 pulse/sec.) travels to the receiver passing through the mud column, the formation and again the mud column. The sonic transmission time between transmitter and individual receivers are as follows.

$$\text{Transmitter} \text{ --- No.1 receiver} : T_1 = T_{m1} + T_{f1} + T_{m2}$$

$$\text{Transmitter} \text{ --- No.2 receiver} : T_2 = T_{m1} + T_{f1} + T_{f2} + T_{m3}$$

Where, T_{m1}, T_{m2}, T_{m3} : sonic transmission time (micro sec/ ft) passing through mud path No.1, 2 and 3.

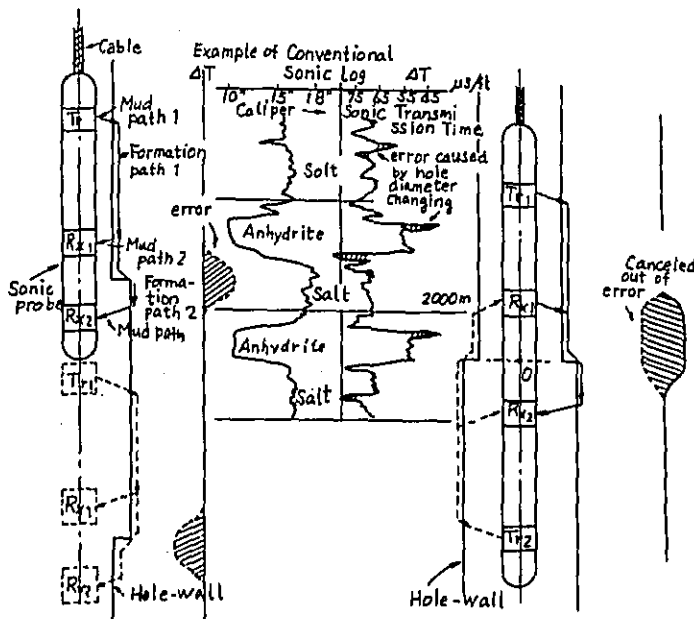


Fig. 12
Principle of Sonic Log.

(a) Conventional sonic log. (b) BHC sonic log

T_{f1} : sonic transmission time passing through formation path No.1.

T_{f2} : sonic transmission time passing through formation path No.2
which is equal to the distance held between receiver No.1 and
No.2.

The sonic log displays a difference between T_2 and T_1 as written below
equation by means of electronics circuit.

$$\Delta T = T_2 - T_1 = T_{f2} + T_{m3} - T_{m2}$$

Since T_{m3} is normally equal to T_{m2} when the hole holds constant diameter
and the probe is set at parallel to the hole axis, then ΔT represents an
actual sonic transmission time of the formation held between receiver No. 1
and No.2. But, the relationship of $T_{m2} = T_{m3}$ is no longer held at the
cases when the hole diameter changes considerably or the probe is not held
at parallel to the hole axis. Then the readings of sonic log include some
error in those cases naturally as shown in the figure.

The new sonic logging system which has double Transmitter -
Receivers system (Transmitter No. 1 - Receiver No.1, No. 2 and Receiver No. 1,
No. 2 - Transmitter No. 2) was developed to cover such shortcomings in the
single Transmitter - Receiver system. The principle of new sonic logging
system will be explained basing on Fig. 12 (b). The geometrical arrange-
ment of the sonic elements is as follows. Transmitter No. 1, Receiver No. 1,
Receiver No. 2 and Transmitter No. 2 are lined up from the top of probe to
down side respectively, and mid point between receiver No. 1 and No. 2 is a
base of vertical symmetry to the upper and down side of double transmitter -
receiver system. When two transmitter are driven by the pulsed current
alternately, ΔT give by the individual Transmitter - Receivers pair are
as follows.

Transmitter No. 1 — Receiver No. 1, No. 2 : $\Delta T_1 = T_{f2} + T_{m3} - T_{m2}$

Transmitter No. 2 — Receiver No. 2, No. 1 : $\Delta T_2 = T_{f2} + T_{m2} - T_{m3}$

Since the equipment achieves the calculation to get an average value of ΔT_1 and ΔT_2 automatically by means of electronics circuit, the value of

$$\Delta T = \frac{\Delta T_1 + \Delta T_2}{2} = T_{f2}$$

represents an actual transmission time of the formation held between two receivers. This type of sonic log is called as BHC Sonic log (Bore - Hole Compensated Sonic Log) and used as a standard sonic log at the present day.

Wylie gave the quantitative relationship between the formation porosity and the sonic transmission time, i.e.,

$$\Delta T = \phi \Delta T_f + (1 - \phi) \Delta T_{ma} \text{ or } \phi = \frac{\Delta T - \Delta T_{ma}}{\Delta T_f - \Delta T_{ma}} \dots\dots\dots(18)$$

Where, ΔT : sonic transmission of formation measured by the sonic log (micro sec/ft).

ΔT_f : sonic transmission time of formation fluids (micro sec/ft), on well compacted formation (formation pressure is held over 6,000 psi), the sonic transmission time of formation fluids is not so much affected by the kind of liquid and its value takes 189 us/ft normally.

ΔT_{ma} : sonic transmission time of matrix (rock).

At the special field where ΔT_{ma} value written in Table II can not be adopted on the calculation of porosity, the following methods are recommendable for determining ΔT_{ma} . Since, on the water bearing clean formation, the relationships of $\phi = (R_w/R_o) 1/2$ or $(R_{mf}/R_{xo}) 1/2$ can be applied into the equation (18) instead of ϕ , the following equations can be obtained.

$$\Delta T = (R_w/R_o) 1/2 (\Delta T_f - \Delta T_{ma}) + \Delta T_{ma}, \text{ or}$$

$$\Delta T = (R_{mf}/R_{xo}) 1/2 (\Delta T_f - \Delta T_{ma}) + \Delta T_{ma} \dots\dots\dots(19)$$

Table II Sonic Velocity of Typical Rocks

Materials	Sonic velocity V _{ma} (ft/sec)	Sonic transmission ΔT_{ma} (us/ft)	Typical value ΔT_{ma} (us/ft)
Sandstones	18,000 to 21,000	55.6 to 47.6	55.5 or 51.0
Limestones	21,000 to 23,000	47.6 to 43.5	47.5
Dolomites	23,000	43.5	43.5
Anhydrite	20,000	50.0	50.0
Salt	15,000	67.0	67.0
Casing (Iron)	17,500	57.0	57.0

Above equations means that the points of cross section between R_w/R_o or R_{mf}/R_{xo} (logarithmic scale on longitude axis) and ΔT (linear scale on abscissa) will drop in an arbitrary line. Therefore, the cross point between an extrapolation of this line and abscissa will be in correspondance with the point of cross plot between $R_w/R_o = 0$ and ΔT_{ma} , because $R_o = \infty$ ($R_w/R_o = 0$) means that the formation is consisted of 100 % rock.

On the hydrocarbon bearing formation, the following relationship will be held between T , R_t and S_w as a same manner as on equation (20).

$$\Delta T = (R_w/R_t) 1/2 (1/S_w) (\Delta T_f - \Delta T_{ma}) + \Delta T_{ma} \dots\dots\dots(21)$$

Fig. 13 is a S_w calculation chart by the use of $\Delta T = (R_w/R_t)$ cross plots based on the equation (21) where $\Delta T_{ma} = 55.5$ us/ft is taken.

POROSITY & SATURATION

from
SONIC & RESISTIVITY LOGS

Consolidated Formations

Read S_w directly for Carbonates.

Multiply S_w by 0.9 for Sandstones.

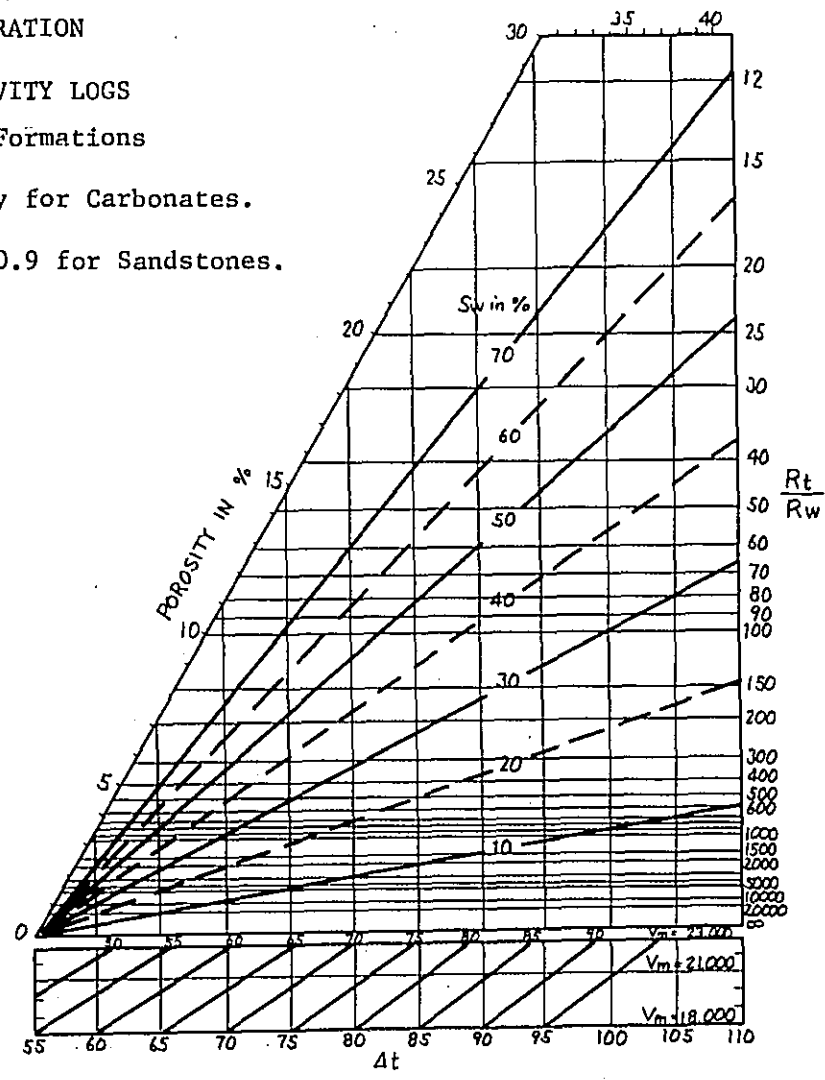


Fig. 13 T - S_w Calculation Chart.

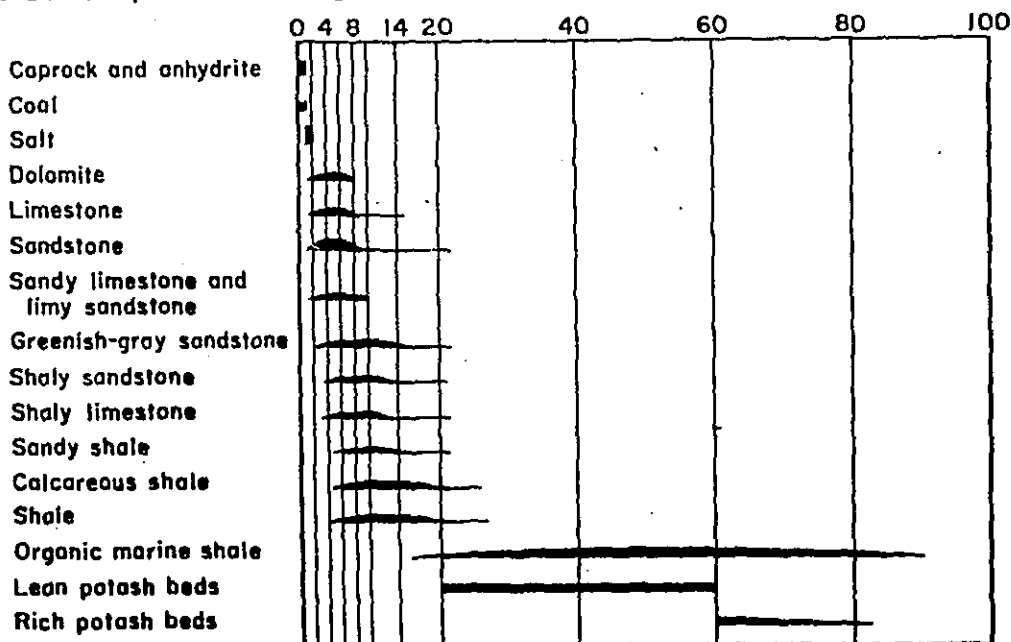
When the formation is not well compacted, formation porosity given by sonic log shows higher value than actual one in general. Then, Wylie proposed that the following compaction correction should be taken into account when the sonic transmission time of the shale adjoining to the interested formation shows over than 100 us/ft.

$$\phi = \frac{100}{C T_{\text{shale}}} \frac{\Delta T - \Delta T_{\text{ma}}}{\Delta T_f - \Delta T_{\text{ma}}}$$

Where, C : compaction factor which holds a value within 1 to 1.5 generally
 ΔT_{shale} : sonic transmission time of shale adjoining to the interested formation.

11. Natural Gamma-ray Log

Fig. 14 is a relative value of radioactivity of the typical rocks. Therefore, the lithological discrimination of formations can be achieved with the help of natural gamma-ray logging data.



Gamma-ray response of sedimentary rocks. From W.L. Russell, "Well Logging by Radioactivity," *Bull. Am. Assoc. Petroleum Geol.*, Vol. 25, No. 9 (1941).

Fig. 14 Relative Radioactivities of Rocks.

Since radioactivities of the shale are much higher than the one of clean formations such as Sandstone, Limestone or Anhydrite etc., the shape of natural gamma-ray log will be analogue to the one of SP log. Therefore, a depth co-relation of the logging cable between at the cased hole and at the bore hole can be achieved by the use of those two logging curves.

On the present equipment, a pulse height analysis of gamma-ray radiated from the formation can be achieved by the use of scintillation gamma-ray detector, and those data are used to the detection of Uranium minerals.

12. Formation Density Log (Gamma - Gamma density log)

It is well known that interactions between a gamma-ray and materials are consisted of Photoelectric effect, Compton scattering and Electron pair production.

Photoelectric effect

o Photoelectric effect

When the gamma-ray with a relatively low energy collides with an electron of atom, that electron escapes from the atom having some energy which is transferred from the gamma-ray and then gamma-ray disappears promptly.

o Compton scattering

When the gamma-ray collides with the electron of atom, the gamma-ray changes the direction of its orbit. On this reaction, the gamma-ray gives a part of its energy to the electron which is put off from the atom by this collision.

o Electron pair production

When the gamma-ray collides with atom, two electrons having + and - charge are produced in the atom. This reaction occurs only when an energy of gamma-ray is higher than 1.02 MeV because the mass energy of electron has 0.51 MeV.

Since a probability which the Compton scattering is occurred in the material is mainly proportional to the density of material. Formation density log measures the formation density by putting the gamma-ray source such as ^{137}Cs or ^{60}Co and the gamma-ray detector into the hole as shown in Fig. 15.

When the gamma-ray source and gamma-ray detector which are held some distance between each others are set in the material having the infinitely large volume, intensity of scattered gamma-ray entering into the detector can be calculated by the use of Boltzmann's transfer function.

$$\nabla^2 f(r) - \frac{f(r)}{L^2} = - \frac{S(r)}{D} \dots\dots\dots(22)$$

Where, $f(r)$: a number flux of photon at the arbitrary point having the distance of r from the gamma-ray source (n/sec. cm^2)

D : diffusion efficiency.

L : diffusion length (cm).

$S(r)$: number of photon produced at the point interesting (n/sec)

When a point source is put into the material having infinitely large volume, the solution of equation (22) is as follows.

$$f(r) = \frac{1}{4} \frac{S}{r^2} \frac{1}{D} \exp. - \frac{r}{L} \dots\dots\dots(23)$$

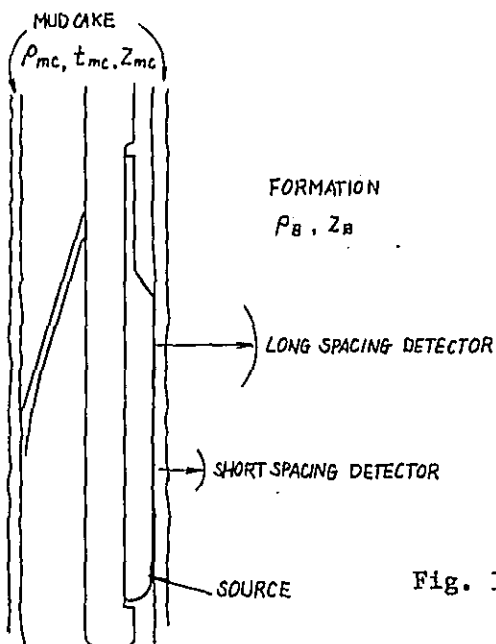


Fig. 15 Diagram of Dual Spacing Formation Density Log.

On the gamma-gamma formation density log, the relationship of $f(r) \propto N_r$ (N_r : count rate of scattered gamma-ray measured by formation density log), $D, L \propto \rho$ are held normally. Therefore, the equation (23) can be re-written as follows.

$$N_r = K \rho \exp. - k\rho \dots\dots\dots(24)$$

Where, K and k are geometrical factors of equipment.

Since the density of sedimentary rock takes the value in the range within 2 to 3.5, the relationship between N_r and ρ might be expressed as,

$$\rho = - A \log N_r + B \dots\dots\dots(24)$$

Where, A and B are constant. Every equipments are so calibrated that A and B take same values for all equipments by the use of the standard pits.

On the recent equipment, two formation density curves are recorded simultaneously by the use of double Gamma-ray source - Detector spacing for compensating the affection of mud cake, because, since the smaller spacing of source - detector will get the more affection of mud cake. Then, the mud cake correction will be achieved with the comparison of data measured by those two source - detector spacings formation density log. Schulumberger calls this type of equipment as FDC tool (Formation Density Compensated tool) and published a mud cake correction chart shown in Fig. 16.

The relation-ship between the formation density and the porosity is given as follows.

$$\rho_b = \phi \rho_f + (1 - \phi) \rho_{ma}, \text{ or } \phi = \frac{\rho_b - \rho_{ma}}{\rho_f - \rho_{ma}} \dots\dots\dots(25)$$

Where, ρ_b : formation density measured by the formation density log.

ρ_f : density of formation water, namely $r = 1$,

ρ_{ma} : density of matrix (rock) which is shown at Table III.

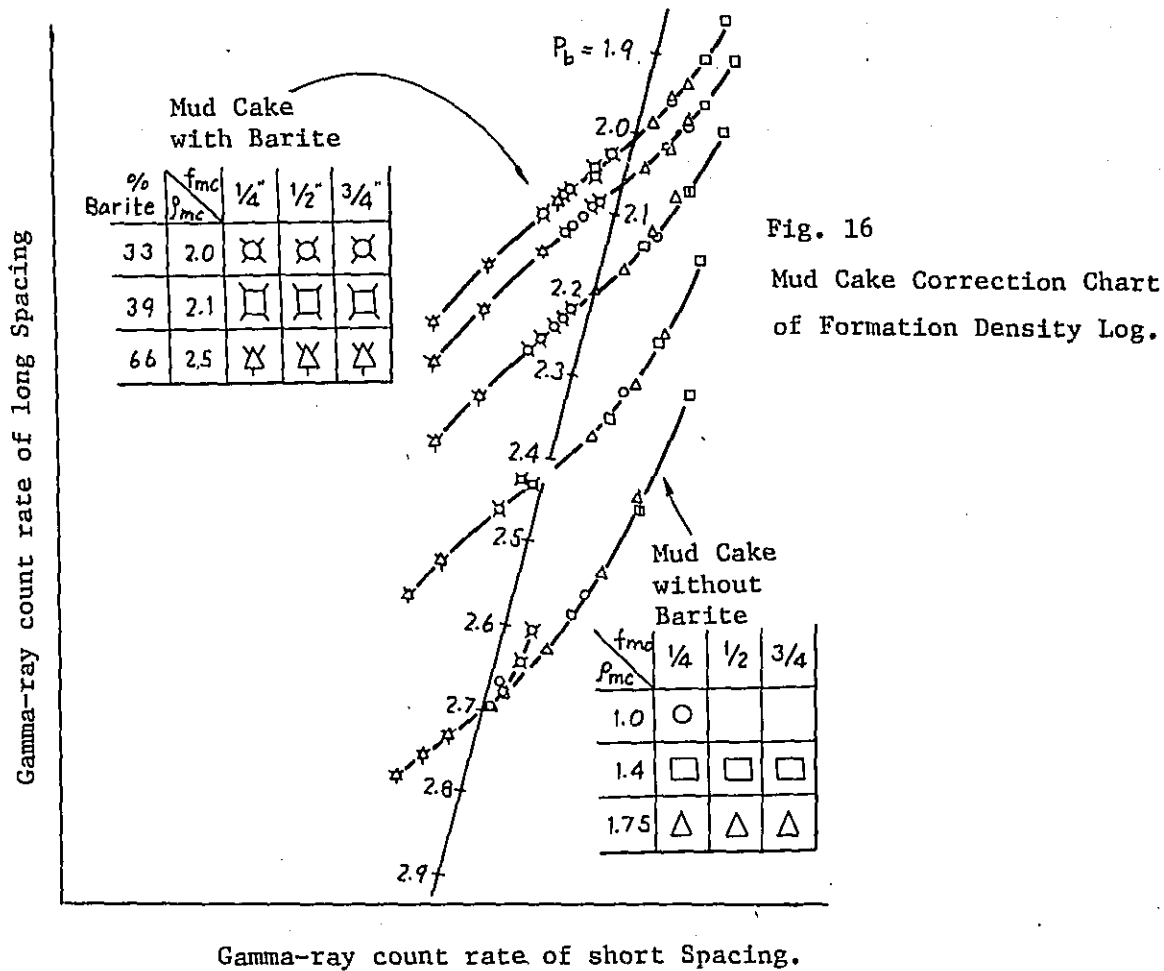


Table III : Density of typical materials

Materials	Components of molecule	Actual density (average)	Values of formation density log
Sandstones	SiO ₂	2.650	2.648
Limestones	CaCO ₃	2.710	2.710
Dolomites	CaCO ₃ MgCO ₃	2.870	2.876
Anhydrite	CaSO ₄	2.960	2.977
Sylvite	KCl	1.984	1.864
Halite (Salt)	NaCl	2.165	2.032
Gypsum	CaSO ₄ 2H ₂ O	2.320	2.351
Anthracite Coal	—	1.400 to 1.800	1.355 to 1.796
Bituminous Coal	—	1.200 to 1.500	1.173 to 1.514
Fresh water	H ₂ O	1.000	1.000
Salt water	200,000 ppm	1.146	1.135
Oil	C _n H _{2n+2}	0.850	0.850
Methane	CH ₄	—	1.335 _b - 0.188

13. Neutron Log

Since hydrogen is a most important atom on the decline of neutron energy when the neutron collides with an atom in the materials, neutron log measures a hydrogen density in the formation by putting a neutron source and detector in the hole. Fast neutron radiated from the neutron source will rapidly be decrease of its energy into the thermal neutron (velocity of neutron is equal to the velocity of gas molecule) when a neutron is injected into the formation which has high hydrogen concentrations. And those thermal neutrons are absorbed by the other atoms such as Cl, Si, etc. which exist at near close to the neutron source, therefore, the number of neutron entering into the neutron detector which is set at some distances from the neutron source is relatively small. While, since the low permeable formation has relatively low hydrogen density, the neutron radiated from neutron source flies relatively long distances in the formation until neutrons become to thermal neutron, therefore, the neutron intensity measured by neutron log shows relatively high values in comparison with the case of high hydrogen densed formation.

J.T. Dewan gave the following relationship between the hydrogen concentrations and the indication of neutron log.

$$N = L \exp. - k (HI) \dots\dots\dots(26)$$

Where, N : number of neutron measured by neutron log.

K, k : geometrical factor of equipment.

(HI) : Hydrogen index of materials.

Since, it is considered that the hydrogen index will be proportional formation porosity in the case which the formation is consisted of the rocks without any clystaline water acompanied, therefore, the equation (26) can be re-written as,

$$N = K \exp. - k \phi, \text{ or } \phi = -A \log N \dots\dots\dots (27)$$

Where, A is a constant and all equipments take same value by calibrations
Fig. 17 is a calculation chart of N - ϕ for different hole diameter.

Since the rocks consisting of formation have some clystaline water, the following correction should be taken into account on the calculation

Pad Epithermal Neutron Porosity Determination

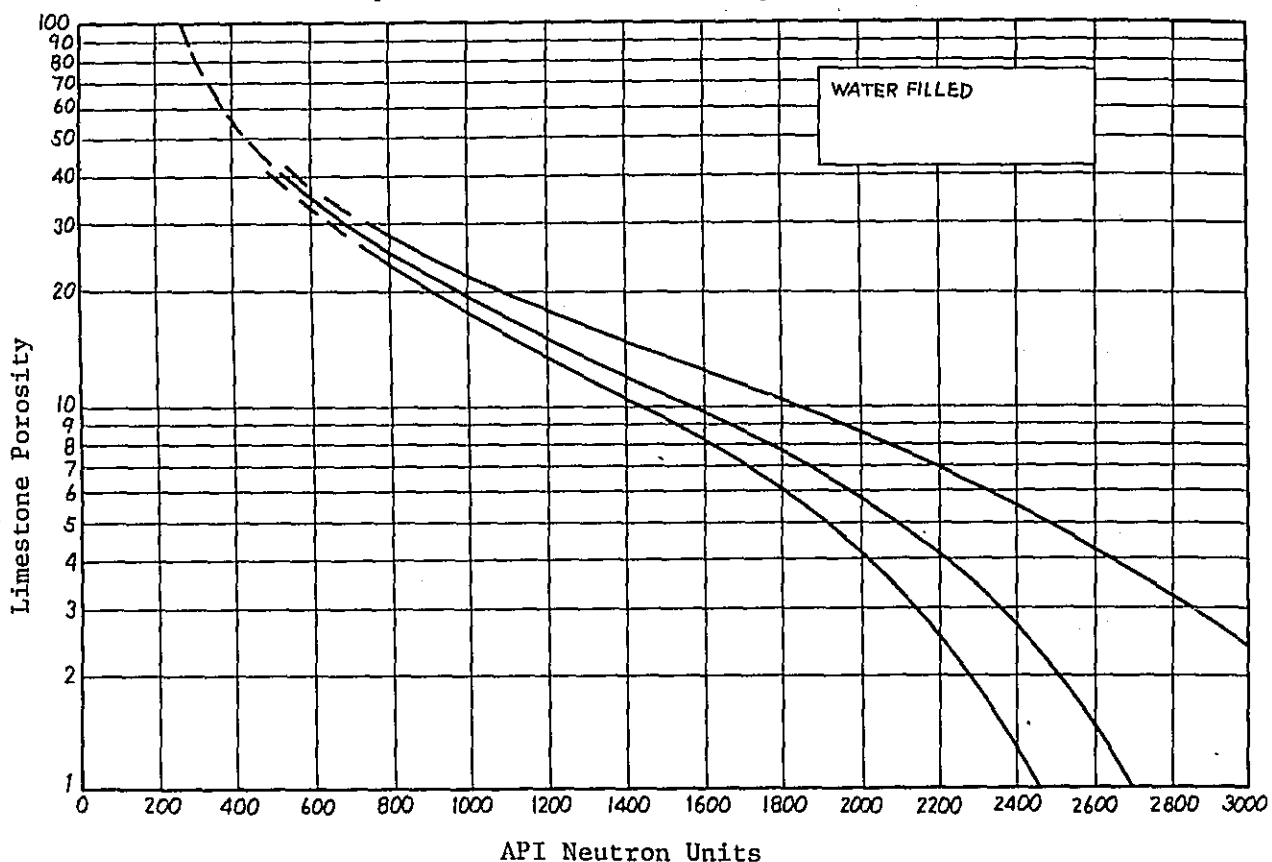


Fig. 17 Neutron Log - ϕ Determination Chart
(for SNP tool)

of neutron porosity.

$$\phi_N = \phi + (1 - \phi) \phi_{ma} , \text{ or } \phi = \frac{\phi_N - \phi_{ma}}{1 - \phi_{ma}} \dots\dots\dots(28)$$

Where, ϕ_N : neutron porosity driven by the use of equation (27).
 ϕ_{ma} : equivalent neutron porosity of the rocks (written in Table IV)

Rable IV : Equivalent neutron porosity of materials.

Materials	Equivalent neutron porosity
	$\phi_{ma} *$
Sandstones $\left(\begin{array}{l} v_{ma} = 18,000 \text{ us/ft} \\ v_{ma} = 19,500 \text{ us/ft} \end{array} \right.$	- 0.035
Limestones	0
$\phi = 5.5 \text{ to } 30 \%$	0.035

Dolomites ($\phi = 1.5$ to 5.5 %, 30 %	0.02
$\phi = 0$ to 1.5 %	0.005
Anhydrite	0
Gypsum	0.49
Salt	0.04
Water	1.00

* This values can only be applied to SNP neutron log (Side Wall Neutron Porosity tool explained at later on)

The life time of thermal neutron in the materials is strongly affected with the macro neutron absorption cross section of the material. In other words, thermal neutrons have far shorter live times in the materials having high neutron absorbing atoms than the one in the material without any neutron absorbing atoms existed. Since a chlorine has high neutron absorption cross section, the readings of neutron log differ between the one measured in salt mud hole and the one measured in flesh mud hole, because the density of neutron in the materials surrounding the probe differs between in those two cases by the reason of the difference of neutron live time even if those two materials have same hydrogen density.

Since densities of epithermal neutron (the energy of neutron is little higher than the one of thermal neutron) in the material are less affected by the neutron life time, i.e., the concentration of NaCl in the material but more affected by the density of hydrogen in the material SNP tool (Side Wall Epithermal Neutron Porosity Tool) having a neutron source and epithermal neutron detector (^3He) in the skid base which is pressed to the hole-wall is now in the practical uses. In recent equipment, two neutron porosity curves are recorded simultaneously by the use of double neutron source - detector spacings for achieving the mud cake correction based on the principles written in the formation density log.

14. Log Interpretation in Shaly Sand.

Since a surface of shale (mudstone) is covered by the negative electron charge as described at SP log, the mudstone has electric conductivity. Therefore, the rules written in the equations (4) and (11) are no longer held on the shaly sand, moreover, SP value in shaly sand decreases in

comparison with the one shown at clean sand because the activity Cl^- ion will be disturbed by those negative charges appeared in the surface of mudstone as shown in Fig. 18. Then, following new log interpretation methods getting the values of S_w and ϕ were proposed for the shaly sand.

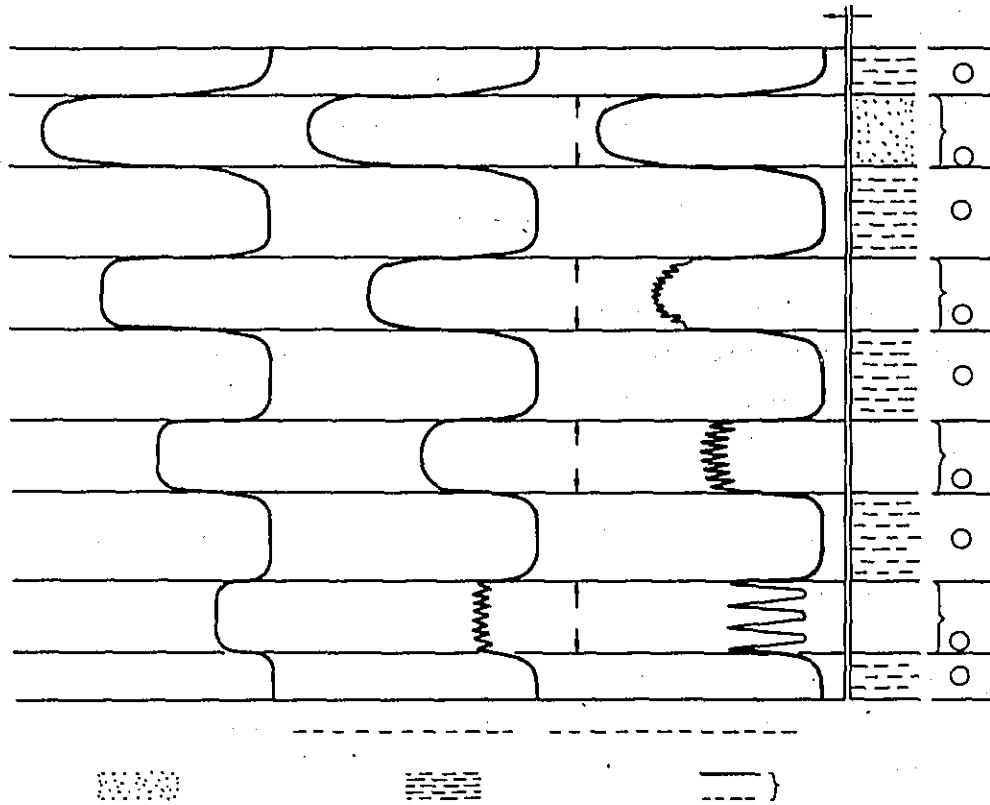


Fig. 18 Example of SP Reduction in Shaly Sand.

1) PSP method

Schulumberger had introduced following equations on the calculation of S_w and ϕ for the shaly sand by the use of = SSP/PSP when the formation is consisted of the alternations of shale streak and sand streak laminated.

$$\left. \begin{aligned} PSP &= -L \log (R_{xo}/R_t) - 2\alpha K \log (S_{xo}/S_w) \\ \alpha &= PSP/SSP \end{aligned} \right\} \dots\dots\dots (29)$$

Where, PSP : SP value shown at shaly sand.
 = PSP/SSP : SP reduction factor.

It is proved that equation (29) is not normally be suitable to the shaly formation of dispersed type.

2) Recent S_w equation for shaly sand

De Witte proposed following equation of S_w calculation for the all type of shaly formations.

$$1/R_t = (V_{sh}/R_c) S_w + (\phi S_w)^2 \cdot 1/R_w \dots\dots\dots(30)$$

Where, V_{sh} : shale concentrations in the formation

R_c : resistivity of mud-stone included in the shaly sand which is represented by $R_c = C.R_{shae}$ normally, where R_{shale} is the resistivity of the shale adjoining to the interested shaly sand and C is a constant depending on the local conditions. C takes between 0.8 to 1.0 in the practical case.

ϕ : formation porosity given by the sonic log, formation density log and neutron log etc.

3) V_{sh} calculations based on the material balanced equation by the help of data given by sonic log, density log and neutron log.

The material balanced equation composed with physical parameters of formation and the data given by the sonic log, density log and neutron log can be formed as follows.

$$\begin{aligned} \Delta T &= \Delta T_f \phi + \Delta T_{sh} V_{sh} + (1 - \phi - V_{sh}) \Delta T_{ma} \\ \rho_b &= \rho_f \phi + \rho_{sh} V_{sh} + (1 - \phi - V_{sh}) \rho_{ma} \dots\dots\dots(31) \\ \phi_N &= \phi + \phi_{N_{sh}} V_{sh} + (1 - \phi - V_{sh}) \phi_{N_{ma}} \end{aligned}$$

Where, $\Delta T, \rho_b, \phi_N$: data given by the sonic log, formation density log and neutron log respectively.

$\rho_f, \rho_{sh}, \rho_{ma}$: density of formation fluid, shale and matrix (rock)

$\phi_{N_{sh}}, \phi_{N_{ma}}$: responses for the neutron log of shale and matrix.

Therefore, ϕ and V_{sh} will be given as the solutions of the simultaneous equation consisted of two of them presented in the equation (31).

List of Figures

- Fig. 1 : Normal resistivity measuring method.
- Fig. 2 : Conventional electrical log.
- Fig. 3 : Principle of Spontaneous Potential.
- Fig. 4 : Chart for deriving the resistivity of electrolyte.
- Fig. 5 : Fluid distributions in the permeable formation.
- Fig. 6 : SSP - $R_{xo}/R_t - S_w$ calculation chart.
- Fig. 7 : Principle of Micro and Micro-latero log.
- Fig. 8 : R_{xo} chart by the use of Micro log.
- Fig. 9 : Principles of Guard electrode log.
- Fig.10 : Principle of Induction log.
- Fig.11 : Geometrical Factor of Induction log.
- Fig.12 : Principle of Sonic log.
- Fig.13 : $T - S_w$ calculation chart.
- Fig.14 : Relative radioactivities of rocks.
- Fig.15 : Diagram of Dual Spacing Formation Density log.
- Fig. 16 : Mud Cake Correction Chart of Formation Density log.
- Fig.17 : Neutron log - ϕ determination chart (for SNP tool).
- Fig.18 : Example of SP reduction in Shaly Sand.

